Available online at www.sciencedirect.com
SCIENCE DIRECT
ELSEVIER
ultramicroscopy
Ultramicroscopy 94 (2003) 283–291
www.elsevier.com/locate/ultramic

Application of evanescent wave optics to the determination of absolute distance in surface force measurements using the atomic force microscope

S.T. Huntington[a,*], P.G. Hartley[b], J. Katsifolis[c]

[a] Particulate Fluids Processing Centre, School of Chemistry, University of Melbourne, Parkville, Vic. 3010, Australia
[b] CSIRO Molecular Science, Vic. 3169, Clayton, Australia
[c] Department of Electronic Engineering, La Trobe University, Bundoora, Vic. 3083, Australia

Received 20 May 2002; received in revised form 2 September 2002

Abstract

A combined scanning near field optical/atomic force microscope (AFM) is used to obtain surface force measurements between a near field sensing tip and a tapered optical fibre surface, whilst simultaneously detecting the intensity of the evanescent field emanating from the fibre. The tapered optical fibre acts as a compliant sample to demonstrate the possible use of the near field intensity measurement system in determining 'real' surface separations from normal AFM surface force measurements at sub-nanometer resolution between deformable surfaces.

Keywords: Optical fibre; AFM; SNOM; High resolution; Distance; Force curves; Evanescent field

1. Introduction

During the past decade there has been an extensive amount of research performed using atomic force microscopy (AFM) with wide-ranging applications. Many experiments focussed on using this technique to measure the forces between native and modified AFM probes and a variety of surfaces, with a particular view to understanding the surface forces operating in colloidal systems [1,2]. A complete understanding of these forces depends on knowledge of both their magnitude and range [1]. In AFM surface force measurements, force magnitudes are measured directly from the deflection of an AFM cantilever, of known spring constant. The range of the surface forces, however, are generally inferred from the region of the measured force-distance profile in which the tip and surface are coupled in their motion, that is, in the 'constant compliance' regime of the data. Whilst for rigid, solid surfaces, the assumption that this region corresponds to zero separation is reasonable, for soft, deformable, or coated samples (i.e. rigid layers) the situation is more complex.

To illustrate this, let us consider the example of a soft polymer on a hard substrate. In this situation, the constant compliance region of the curve may represent either the contact position of

*Corresponding author.
E-mail address: shaneth@unimelb.edu.au (S.T. Huntington).

0304-3991/03/$ - see front matter © 2002 Elsevier Science B.V. All rights reserved.
PII: S0304-3991(02)00338-8

the hard substrate surface (the 'true' zero separation position), or the position at which the elastic modulus of the polymer layer exceeds the spring constant of the AFM cantilever. In this latter case, the compressed layer thickness of the polymer cannot be retrieved from the force versus distance profile, since the absolute tip–substrate separation is not independently measurable.

Polymer layers are frequently employed as flocculent or dispersant coatings in colloidal systems, where surface forces due to polymer extension into solution are thought to be major determinants of their operational efficacy [3]. Accurate measurement of polymer layer extension into solution, in conjunction with surface force measurements is thus extremely desirable in the study of the mode of action of such coatings, and further in the rational design of future coating systems.

Currently, the surface force apparatus and total internal reflectance microscope (TIRM) [1,4] are the pre-eminent techniques capable of performing such measurements. The surface force apparatus in particular has provided a wealth of excellent information regarding a number of adsorbed polymers and other systems [5,6]. However the technique is somewhat cumbersome in operation, and limited in flexibility as regards substrate material composition.

In this paper, we demonstrate a new technique, based on the simultaneous acquisition of surface force and near field optical intensity data, which enables compliant samples to be readily examined with exceptional signal to noise characteristics and, in principle, for the 'real' separation between a probe and substrate surface to be measured in the presence of adlayers. The technique utilises scanning near field optical microscopy (SNOM) cantilevered probes to detect the decay characteristics of an evanescent field while simultaneously operating in deflection mode.

In the simplest case, we can investigate the requirements for a field to be considered evanescent by looking at a ray incident on the interface of two dielectric media, with indices n_1 and n_2 (see Fig. 1). For the special case where the incident ray, k, satisfies the conditions for total internal reflection, there will be a corresponding reflected ray k_1 and a second ray k_2 which would normally be the refracted ray, but for angles less than the critical angle only carries energy parallel to the interface.

If the angle of incidence θ is greater than the critical angle, then the field in the second medium will be an evanescent wave of the form [7]

$$E(x) = E_0 \exp\left(-\frac{\omega x \gamma}{v_2}\right) \exp\left[\mathrm{i}\omega\left(\frac{z n_1 \sin\theta}{n_2 v_2} - \omega t\right)\right],$$

where ω is the angular frequency, v_2 is the speed of light in medium 2 and $\gamma \equiv \sqrt{(n_1^2 \sin^2\theta / n_2^2) - 1}$. This represents the case where the wave is travelling in the z-direction and is exponentially attenuated in the x direction. The intensity of the wave is thus given by

$$I(x) = I_0 \exp\left(-\frac{2\omega x \gamma}{v_2}\right).$$

In this paper, we utilise a system that produces an evanescent field of this type.

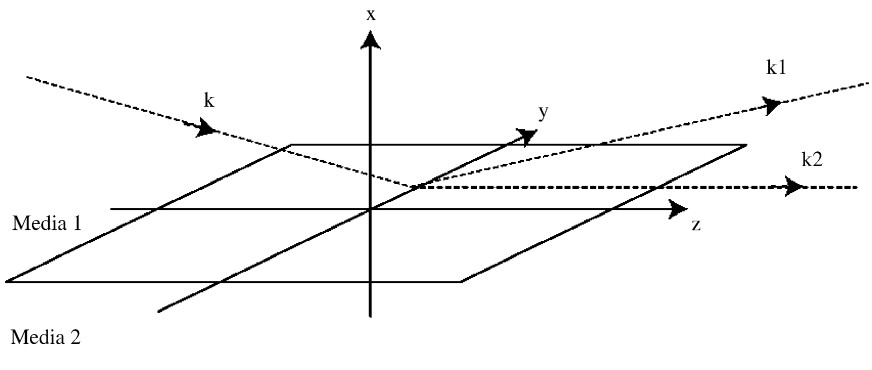

Fig. 1. Schematic of a single ray reflection between two dielectric surfaces.

2. Experiment

The system used in these experiments is a combined AFM/SNOM system. A commercial AFM (Digital Instruments—Dimension 3100) was modified to allow commercial cantilevered optical fibre SNOM probes to be utilised (Nanonics Inc.). The probes consist of a bent and tapered silica optical fibre, coated in chromium, with an aperture approximately 50 nm in diameter. The chromium coating makes the fibres robust and readily reusable both in contact and intermittent contact mode. Light collected by the aperture is transmitted along the fibre to a photomultiplier tube (Hamamatsu R928) for detection. The signal is then amplified and recorded via the DI control computer 'auxiliary in' voltage acquisition channel. In this configuration the SNOM system is said to be operating in collection mode, and the system is capable of simultaneously collecting optical and cantilever tip deflection data. In this study, an optical fibre taper sensor was used as a sample substrate (see Fig. 2). This sensor consists of a standard piece of optical fibre that has had its diameter radically reduced in a small region. In the bulk fibre, the optical mode is located well within the fibre. In the tapered region, the fibre has such a small diameter that part of the optical field travels outside the fibre in the form of an evanescent field. This field moves along the fibre axis, but decays exponentially with radial distance from the fibre. Generally, such fibres are employed as sensors, by immersing the tapered region into a solution and allowing the evanescent field emanating from the fibre surface to interact with the solution. The light losses from the fibre incurred are monitored, and changes in the solution can be readily measured. For our experiment, the taper is an excellent

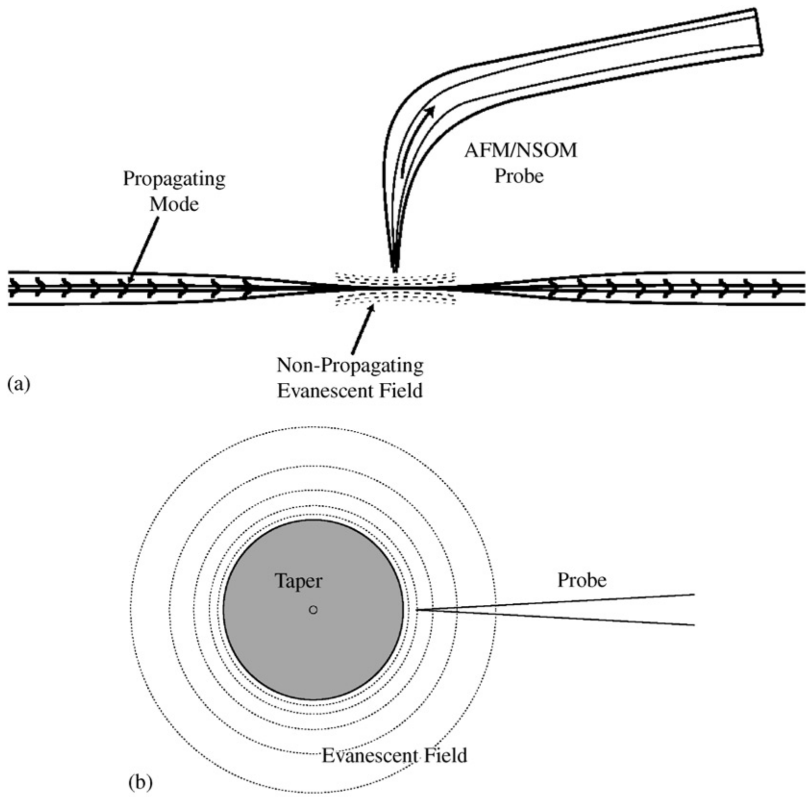

Fig. 2. (a) Schematic of the near field optical probe above the evanescent field generated by an optical fibre taper sensor. (b) Cross section of fibre taper showing orientation of fibre probe tip for evanescent field measurements.

source of a strong evanescent field that has been well characterised previously [8]. Light of wavelength 532 nm is coupled into the taper system from a 100 mW, frequency doubled diode pumped CW laser.

In addition, we require a sample that will normally be difficult to measure due to its compliant nature. The fibre taper consists of a 10 μm wide cylindrical piece of glass subtended from two points approximately 5 cm apart. The small size of the taper in combination with its flexibility and poor supports makes it extremely compliant.

The cantilevered SNOM probe is aligned optically so that the tip sits above the centre of the taper. The AFM piezo system is then used to drive the probe towards the sample and simultaneous deflection force curves and evanescent field maps are collected.

Surface force measurement data was acquired simultaneously to the acquisition of optical intensity data. Here, the deflection of the SNOM tip was monitored as a function of the displacement applied to the tip by the driving piezoelectric element.

In order to present the surface force measurements in the accepted form of force versus separation, measured tip displacement voltages were converted to actual displacements (nm) using the internal 'constant compliance line' slopes (V/nm) from the surface force measurements (retract curves, see Fig. 3). Ideally, the compliance line slope should be obtained from measurements against a flat rigid surface, however this step was omitted for the current pilot study. The reader is warned that this may represent a significant inaccuracy in the surface force measurements presented here. The spring constant of the SNOM tip was also not measured in the current study, and deflection data was converted to force using the manufacturers nominal spring constant of 0.5 N/m. This may lead to another significant inaccuracy in the data presented, however neither of these omissions impact on the conclusions of this study. The SNOM probe spring constant can be obtained using existing techniques for AFM probes such as the added mass method should it be required for specific measurements.

In order to present the optical intensity data in conjunction with the surface force measurements, the intensity data which corresponded to each separation position calculated from the line of constant compliance in the surface force measurements (see above) was plotted.

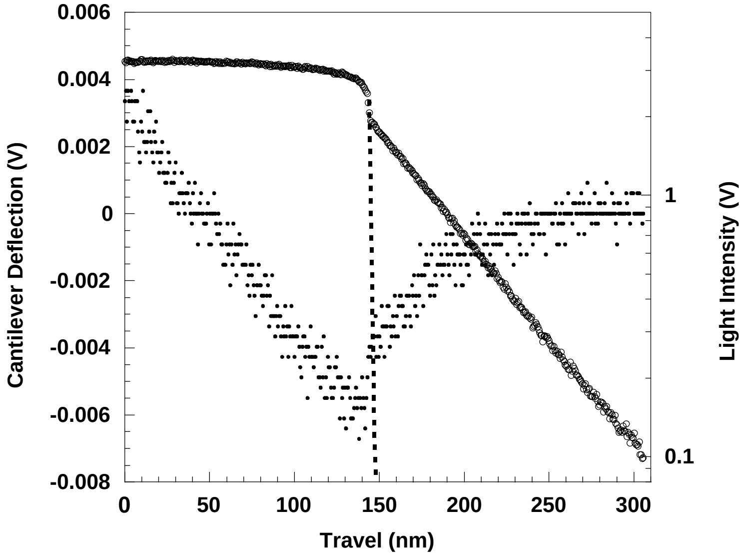

Fig. 3. Raw data recorded during approach of Near Field tip to fibre surface. The dotted line indicates the contact position as derived from the jump in near field intensity (see text for details): ● Tip Deflection Measurements; ° Near Field Intensity Measurements.

3. Results and discussion

Fig. 3 shows an example of 'raw' cantilever deflection and near field intensity data recorded as a near field tip approached the fibre taper sample. The standard features of the force curve are all visible in Fig. 3, such as the long range zero deflection regime, an attractive force regime denoted by a downward deflection of the tip, followed by an inward 'jump' into contact, a linear 'constant compliance region' is then observed. The near-field intensity data also shows the expected form, namely an exponential increase in intensity as the tip moves through the evanescent field emanating from the fibre, and finally a plateau maximum signal, corresponding to the tip and fibre being coupled. Between these two regimes, however, there also exists a slight 'kink' in the optical intensity data. This region is of interest, since it likely denotes a changing geometry of interaction between the tip and the surface as the tip is pushed against the fibre. This is an important observation, since any change in the geometry of the interaction could have important implications for interpretation of surface force measurement data. It is worthy of note that the signal to noise level in the approach to the sample is considerably higher than that found in the deflection data set.

A key feature of the near field intensity plot is a discontinuity in the data at ca. 145 nm travel. This discontinuity corresponds to an inward jump of the tip towards the fibre surface (as observed in the deflection data), resulting in a sudden intensity increase due to contact between the tip and the fibre. The entire 'jump to contact' event occurs in this case within a 3 nm change in piezo drive travel in the optical intensity data plot. This is in comparison to the deflection data, where the jump into contact region can only be resolved within a ~ 12 nm travel window. This is an important feature, since it provides evidence that the near-field intensity data has a higher degree of sensitivity to separation between the tip and the surface than the deflection measurements. This feature will be discussed in more detail later.

Fig. 4 shows the analogous data to Fig. 3, recorded during retraction of the tip from the fibre taper. In this case, the surface force measurement shows a much clearer discontinuity, which results from the tip and fibre detaching as the adhesion between them is overcome. Once again, a drop in the optical intensity data occurs at precisely the same position.

The clarity of the discontinuities in the optical intensity data in comparison with the 'jumps' in the deflection data leads us to an interesting possibility: namely that the intensity discontinuities may be used to define a 'true' zero separation between the tip and surface in the surface force measurements

The data in Figs. 5 and 6 have been processed incorporating this assumption. Here, a constant compliance line slope has been derived from the retraction deflection data (Fig. 3, 0–200 nm portion), and the photodiode response calibrated such that the piezo travel (x-axis, Figs. 3 and 4) may be converted to 'relative separation'. This could also be achieved in a closed loop z-axis system by utilising the exponential form of the field decay and calculating distortions in position from the measurement of this field. Force curves have only been included to contrast the signal to noise of the two detection systems.

In addition, force has been calculated from the deflection data, using this relationship between photodiode output and actual tip displacement, by multiplying the measured tip displacement by the spring constant of the near field sensing tip, 0.5 N/m. We note that this approach assumes a non-compliant surface, which the fibre taper clearly is not. In a 'real' measurement, the relationship would be derived by performing an initial measurement of the interaction between the tip and a rigid surface, however for reasons of experimental complexity, this step was not performed in the current study. The zero position in these data sets is derived from the discontinuities in the optical intensity data, and both the optical intensity and force data sets have been scaled to these positions.

The key features of note from Figs. 5 and 6, are the remarkable agreement between the optical intensity and deflection data sets with regards to the positions of the 'jumps' (inwards and outwards), as well as the long range detection of the proximity of the fibre surface using the optical

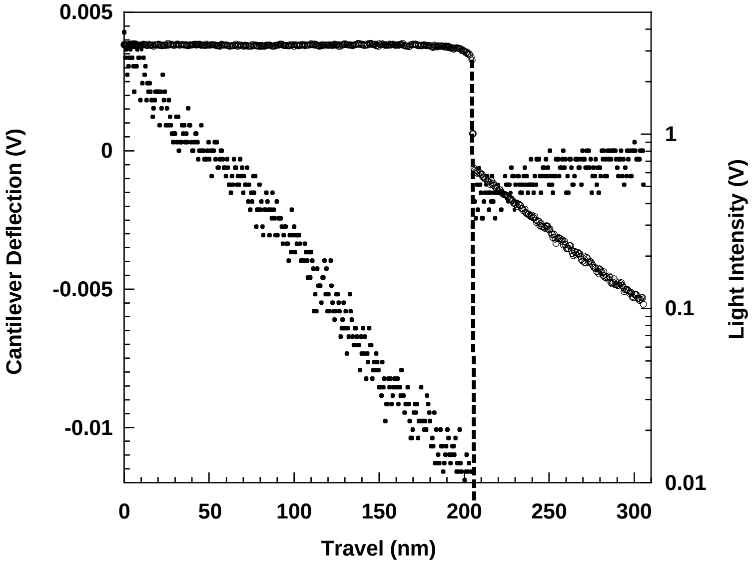

Fig. 4. Raw data recorded during retraction of Near Field tip from fibre surface. The dotted line indicates the detachment position as derived from the jump in near field intensity (see text for details): • Tip Deflection Measurements; ◦ Near Field Intensity Measurements.

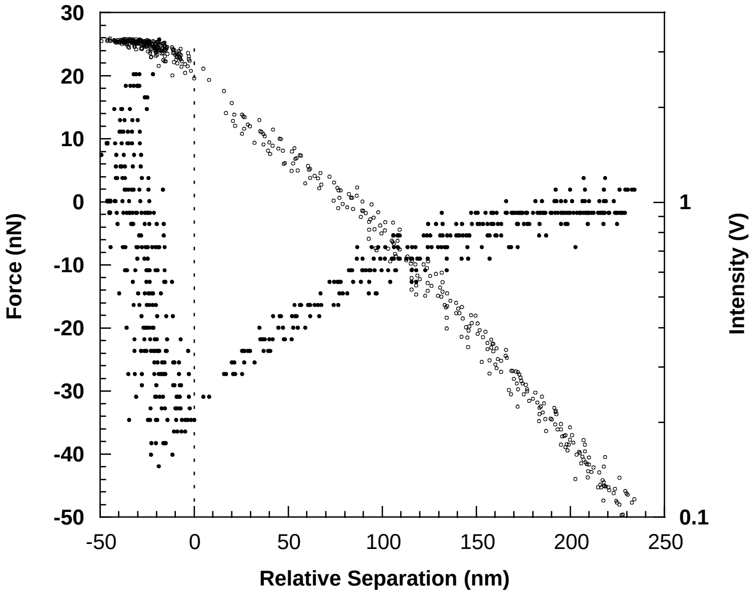

Fig. 5. Scaled Force/Near Field Intensity for approach of Near Field tip to fiber surface using constant compliance line derived from deflection data (Fig. 3), and zero separation position derived from near field intensity data (see text for details): • Tip Deflection Measurements; ◦ Near Field Intensity Measurements.

intensity measurement. This exceeds 200 nm in both the approach and retract directions. This points to another possible application of the near field detection system, that of providing a high sensitivity feedback signal for maintaining the tip above a sample of interest. This feature could have

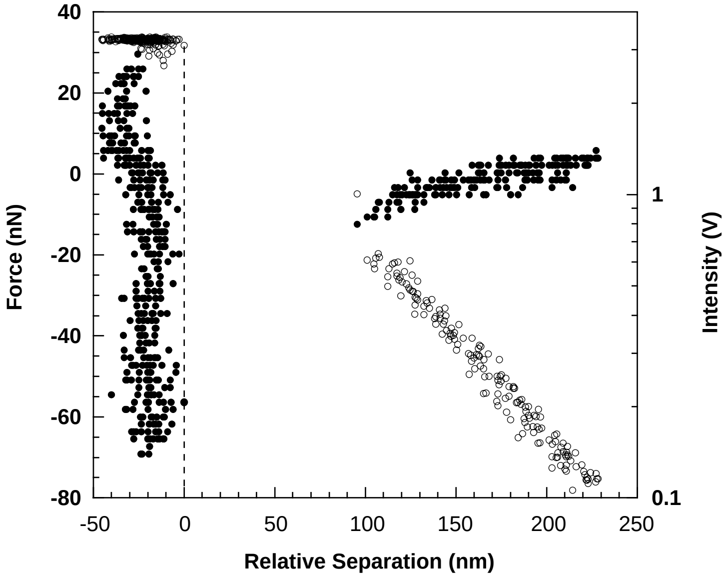

Fig. 6. Scaled Force/Near Field Intensity for retraction of Near Field tip from fiber surface using constant compliance line derived from deflection data (Fig. 3) and zero separation position derived from detachment point from near field intensity data (see text for details): ● Tip Deflection Measurements; ° Near Field Intensity Measurements.

a great deal of interest in, for example, 'soft contact imaging' of surface-adsorbed aggregate structures. The optical signal detected can be readily increased further if the signal to noise level is not sufficient. In our experiments, we used a poor coupling efficiency from the source laser that was easily adjustable. Fig. 7 shows the almost complete lack of hysteresis in the optical intensity data in approach and retraction.

In addition to the 1-dimensional evanescent field (z-axis), it is important to consider the 2-dimensional evanescent field (x–y plane) to determine the quality of the taper in use and whether or not it would be useful in the case for force-curve arrays where a large number of curves are built up over an area to map the interaction between the tip and the surface. To achieve this the sample was scanned in a plane above the taper. The scan in this case is a strip 76 μm × 10 μm. Fig. 8 shows the result of this scan. The evanescent field regions in this case are highly complex, indicating that even though the stock fibre used is single mode at the operating wavelength, the tapered region itself supports a number of modes. This particular taper is therefore not suitable for use in two-dimensional force work. The modal characteristics of tapers are readily variable via their size and index, this coupled with their exceptional power throughput make them good candidates for future work.

Even more ideal than the fibre taper are structures that contain a planar geometry that support an evanescent field. In this category there are three devices of particular interest; the planar waveguide structure, standard optical prisms and the D-shaped optical fibre sensor. All three provide flat silica surfaces above which exists a strong evanescent field. For the D-shaped optical fibre and the planar waveguide structures, the field is relatively constant over a lateral range of several microns. In actuality the lateral field distribution depends on the size of the guiding region within the device, and typically drops to zero beyond a range of 5–10 μm. Fig. 9 shows the field distribution above the core of a D-shaped optical fibre. This image also demonstrates the strength of the SNOM probe used, as there is no change in optical intensity as a result of continued contact and lateral motion on the sample. The field structure above buried planar waveguides has been previously measured [9] indicating similar field

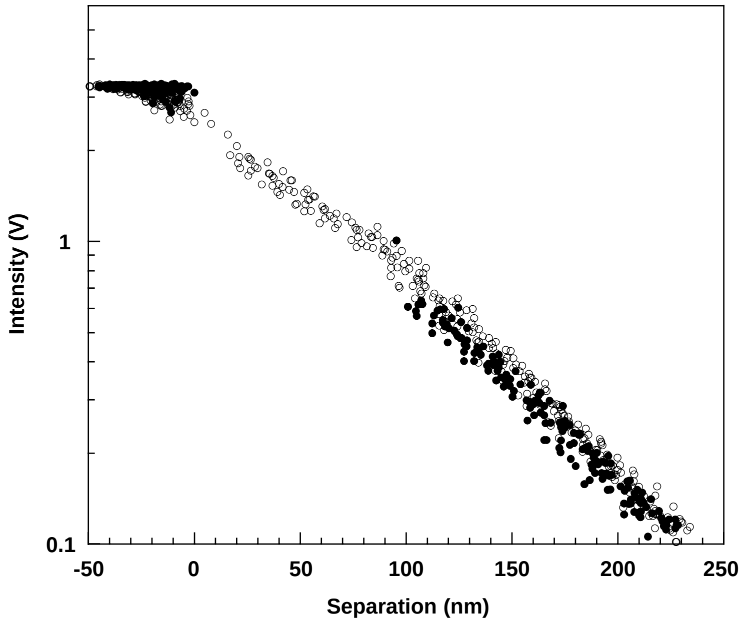

Fig. 7. Lack of hysteresis in scaled near field intensity approach and retract data: ● Retract Data; ° Approach Data.

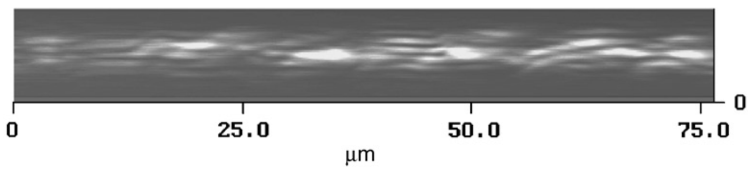

Fig. 8. 2D near field image of the evanescent field structure in a plane directly above the optical fibre taper. The complex mode structure within the taper is clearly visible.

distribution. It should be noted that for the type of system suggested in this paper, buried channel waveguides should be replaced with surface waveguides. The reason for this is that most experiments in this field are performed in solution, and the presence of index values of 1.33 (water) or higher above the waveguide region will prevent excess loss from the waveguide. Such a structure however would not be suitable for use in air or vacuum. Waveguide structures also provide a rigid, non-complient substrate which are far more applicable for most experiments that the test fibre used in this paper. It should be noted that the fibre taper was only utilised as it provide simple evanescent field source that was also complient. Even in the presence of adlayers, the field will exhibit evanescent decay properties in the direction perpendicular to the optical propagation axis, with decay parameters specific to the entire region index profile (waveguide, adlayer, external medium and probe).

4. Conclusions

An optical analogue to a conventional atomic force microscopy force curve has been demonstrated. This system has been shown to have a signal to noise level an order of magnitude better than conventional systems. The jump to contact point has been located with an accuracy of 0.5 nm for a compliant sample and the actual contact point shown to be within 3 nm of this point. In addition the use of evanescent fields in this way

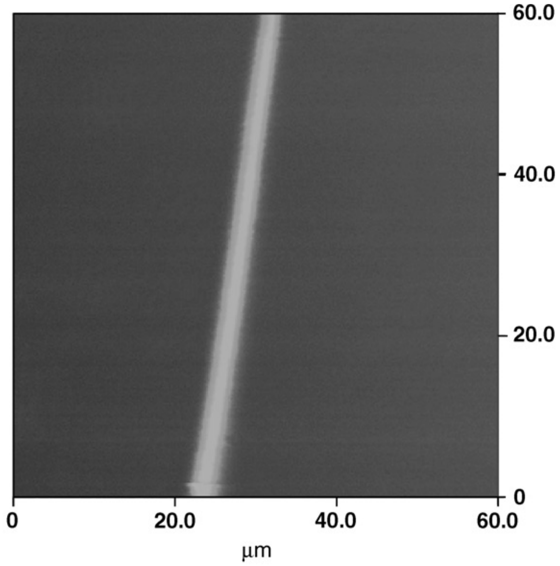

Fig. 9. 2D near field image of the evanescent field structure in a plane directly above the flat face of a D-shaped optical fibre.

provide a measure for determining the range to contact out to a distance of > 200 nm. The experiments suggest that a combined near field optical–surface force microscope could allow the unambiguous determination of separation between a probe and compliant/deformable surface, such as a liquid–liquid interface [10], as at this point the optical power will be constant despite further piezo motion.

Acknowledgements

The support of the Australian Research Council (SH), and the Australian Photonics Cooperative Research Centre is acknowledged.

References

[1] J.N. Israelachvili, Intermolecular and Surface Forces, 2nd Edition, Academic Press, London, 1992.
[2] W.A. Ducker, T.J. Senden, R.M. Pashley, Nature 353 (1991) 239–241.
[3] G.J. Fleer, M.A. Cohen Stuart, J.M.H.M. Scheutjens, T. Cosgrove, B. Vincent, Polymers at Interfaces, 1st Edition, Chapman & Hall, London, 1993.
[4] M.A. Bevan, D.C. Prieve, Langmuir 16 (24) (2000) 9274–9281.
[5] P.F. Luckham, B. Costello, Adv. Colloid Interface Sci. 44 (1993) 183–240.
[6] T. Ederth, V. Bergeron, M.W. Rutland, Adv. Colloid Interface Sci. 67 (1996) 119–183.
[7] M. Born, E. Wolf, Principles of Optics, 6th Edition, Pergamon Press, Oxford, 1980.
[8] S.T. Huntington, J. Katsifolis, P.N. Moar, P. Mulvaney, A. Roberts, L.W. Cahill, K.A. Nugent, IEE Proc. Optoelectron. 146 (5) (1999) 239–243.
[9] G.H. Rhodes, B.B. Goldberg, M.S. Unlu, S.T. Chu, W. Pan, Y. Kokobun, B.E. Little, Appl. Phys. Lett. 75 (16) (1999) 2368–2370.
[10] P.G. Hartley, F. Grieser, P. Mulvaney, G.W. Stevens, Langmuir 15 (1999) 7282–7289.